

CARRIER-ENVELOPE-PHASE STABLE LINEARLY AND CIRCULARLY POLARIZED ATTOSECOND PULSE SOURCES

Z. Tibai[#], Zs. Nagy-Csiha, G. Almási, J. Hebling, Institute of Physics, University of Pécs, Hungary
 Gy. Tóth, J.A. Fülöp, MTA-PTE High Field Terahertz Research Group, 7624 Pécs, Hungary

Abstract

We recently proposed a robust method for producing few-cycle attosecond pulse generation in the extreme ultraviolet spectral range. It is based on radiation of relativistic ultrathin electron layers, which are produced with inverse free electron laser process. In the present article the energy of this attosecond source is investigated numerically for the linearly and circularly polarized cases.

INTRODUCTION

In recent years a few phenomenon depending on carrier-envelope-phase (CEP) was recognized [1]. Waveform-controlled few-cycle laser pulses enabled the generation of isolated attosecond pulses and their application to the study of electron dynamics in atoms, molecules, and solids [2].

EUV pump—EUV probe experiments can be carried out at free-electron lasers (FELs) [3,4]; however, the temporal resolution is limited to the fs regime. Various schemes, such as the longitudinal space charge amplifier [5], or two-color enhanced self-amplified spontaneous emission (SASE) [6] were proposed for attosecond pulse generation at FELs. A very recent scheme suggests possible generation of sub-attosecond pulses in the hard X-ray region [7]. But the stochastic pulse shape is disadvantageous; furthermore there are no reliable techniques available for CEP control of attosecond pulses. Recently we proposed a robust method for producing waveform- and CEP-controlled attosecond pulses in the EUV spectral range [8]. Here we investigate numerically the feasibility and stability of this technique.

SIMPLE SETUP

Our proposed setup is shown in Fig. 1. A relativistic electron beam e.g. from a LINAC is sent through a modulator undulator (MU) where a TW-power laser beam is superimposed on it in order to generate nanobunches by the inverse free-electron laser (IFEL) action. The nanobunched electron beam then passes through a radiator undulator (RU) consisting of a single or a few periods. The radiator undulator is placed behind the modulator undulator at a position where the nanobunch length is shortest. Of course, efficient coherent radiation generation is possible only if the nanobunch length is shorter than the half period of the radiation.

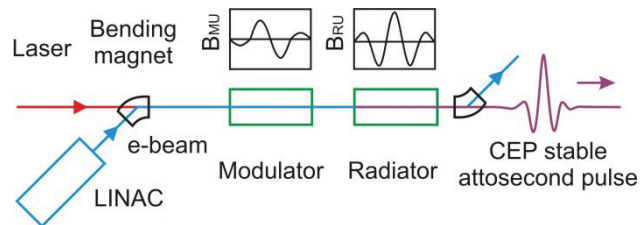


Figure 1: Layout of the setup.

SIMULATION METHOD

The General Particle Tracer (GPT) [9] numerical code was used for simulation of nanobunching in the modulator undulator. In the simulations the parameters of the electron bunch before the nanobunching were chosen according to published parameters of the electron bunches created by the accelerator of FLASH at DESY, Germany (Table 1) [10,11]. Electron bunches with 60 μm transversal size were assumed.

Table 1: Parameters used in the Simulations

Parameter	Value
E -beam energy (γ)	2000
E -beam charge	250 pC
E -beam energy spread (1σ)	0.05 %
E -beam Normalized emittance	1.4 mm mrad

Inside the modulator undulator the interaction between the electrons, the magnetic field of the undulator, and the electromagnetic field of the modulator laser with 516 nm wavelength and 10 TW power (P_L) introduces a periodic energy modulation of the electrons. This energy modulation leads to the formation of nanobunches in the drift space behind the MU. The charge of a single nanobunch is 1.0 pC and according to the simulations, its length can be as short as 6 nm (at 4.9 m behind the center of the modulator undulator).

The temporal shape of the ultrashort pulses emitted by these extremely short electron nanobunches in the RU, were calculated at a plane 8 m behind the middle of the RU.

The wavelength of the EUV radiation (λ_r) is determined by the well-known resonance condition:

$$\lambda_r = \frac{\lambda_{RU} \left(1 + \frac{K_{RU}^2}{2} \right)}{2\gamma^2}, \quad (1)$$

[#]tibai@fizika.ttk.pte.hu

where λ_{RU} is the period of the RU, $K_{RU} = eB_0\lambda_{RU}/2\pi mc$ is the undulator parameter, B_0 is the peak magnetic field of the RU, e and m are the electron charge and mass, respectively, γ is the relativistic factor, and c is the speed of light.

The EUV radiation waveform is determined by the magnetic field distribution of the RU along the electron beam propagation direction (z). The magnetic field distribution of the RU is given by Eq. 2 for linearly polarized case:

$$B_{RU} = B_0 \cdot \exp\left(-\frac{z^2}{2\sigma^2}\right) \cos\left(\frac{2\pi z}{\lambda_{RU}}\right), \quad (2)$$

if $-\frac{L}{2} < z < \frac{L}{2}$, otherwise 0,

where σ is the standard deviation of the Gauss envelope and L is the length of the RU. These parameters were set to $\sigma = 1.5/\sqrt{4\ln(2)}\lambda_{RU}$ (the FWHM of the envelope of the magnetic field is $1.5\lambda_{RU}$) and $L = 2.5\lambda_{RU}$ [8,12]. Similarly, magnetic field distribution of the RU in the circularly polarized case was described in [13].

EUV PULSE GENERATION AND RESULTS

The simulated waveform of the generated EUV pulses closely resembles the magnetic field of the RU (Eq. 2) [14]. The shapes of the pulses for different modulator laser pulse powers – for constant spot sizes, while the peak electric field was varied – are shown in Fig 2. The period length (42.7 cm) of the RU was chosen so that the radiation wavelength was 60 nm for $K = 0.5$ undulator parameter according to Eq. (1). The peak electric field of the generated attosecond pulse is 2.5 MV/cm for 2 TW and 3.2 MV/cm for 10 TW modulator laser power, respectively. The reason of the lower EUV intensity for lower modulator laser power is that lower laser power

results lower energy-modulation in electron bunch and the drift space will be longer. Therefore, the transversal sizes of the nanobunches are bigger for lower laser power and the solid angle of radiated field decreases [8]. As it expected, the temporal shapes of radiated electric fields are CEP stable and the shape is practically independent of the power of the modulator laser pulse.

The EUV pulse energy as a function of the radiation wavelength in the range of 20-200 nm – calculated at different modulator laser powers for $\gamma = 2000$ and $K = 0.5$ – is shown in Fig. 3. The radiation wavelength, given by the resonance condition Eq. (1), can be set by the choice of the RU period λ_{RU} . The pulse energy first increases with increasing the wavelength. This range is followed by saturation at the 10 TW case and a subsequent energy decrease (blue line in Fig. 3) for the longest wavelength. The reason of the latter is that longer undulator periods are needed to generate longer wavelengths. Due to the associated longer path inside the RU the average nanobunch length increases and creates two separated nanobunch from each other, thereby reducing coherence in the radiation process. For lower powers the average length of the nanobunch does not increase as fast as for 10 TW, therefore there the energy increases with increasing the wavelength on the whole investigated EUV wavelength range.

According to the calculations, single-cycle EUV pulses with 50, 86, 111, and 134 nJ energy can be generated at $\lambda_r = 60$ nm for 2, 4, 6 and 10 TW modulator laser powers, respectively.

In another series of calculations the wavelength of the modulator laser power was varied (516, 800 and 1032 nm). The EUV pulse energy as a function of the radiation wavelength in the range of 20-220 nm (similarly to Fig. 3) for $\gamma = 2000$, $P_L = 10$ TW and $K = 0.5$ is shown in Fig. 4.

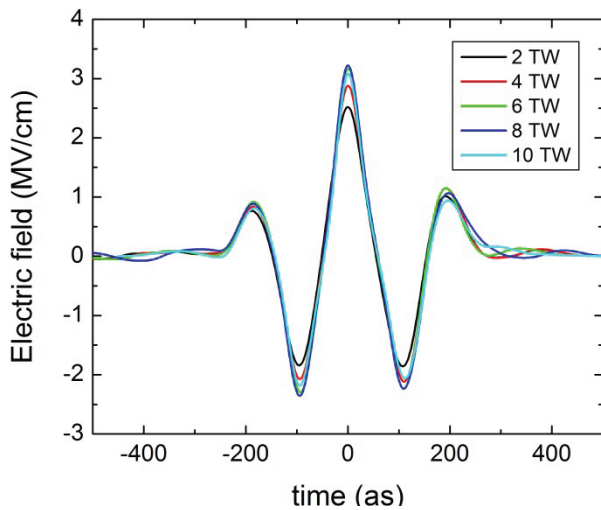


Figure 2: The temporal shape of the electric field of the EUV pulse for different modulator laser powers.

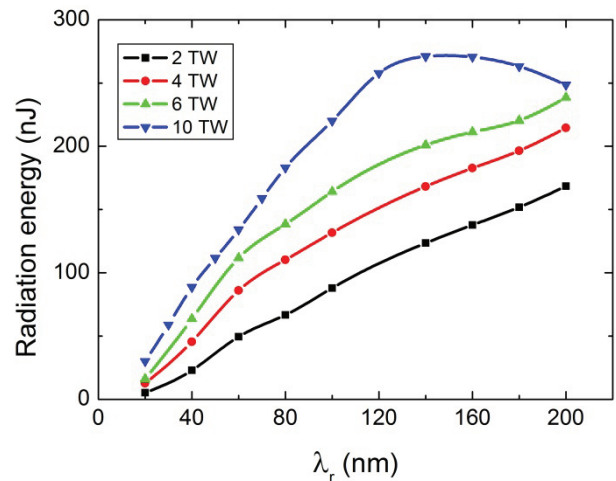


Figure 3: Dependence of the EUV pulse energy on the wavelength of the generated pulses.

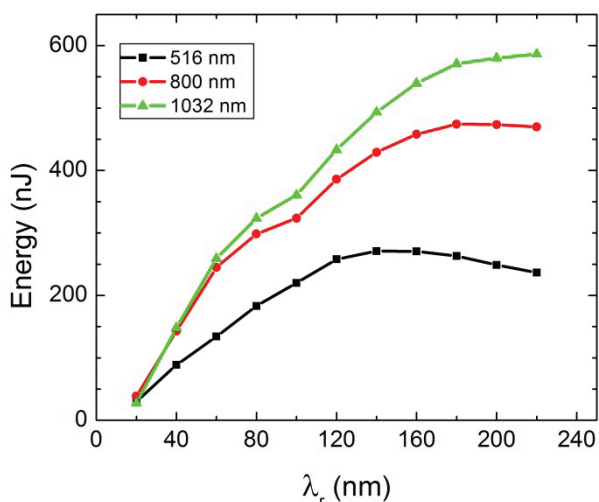


Figure 4: Dependence of the EUV pulse energy on the radiation wavelength for $\gamma=2000$ and $P_L = 10$ TW and three different modulation laser wavelengths.

The largest EUV pulse energy is obtained with the longest modulator laser wavelength. Certainly, the energy of the EUV pulse depends on the charge of the nanobunch. Using longer modulator laser it is possible to concentrate larger charge in a nanobunch. We note, however, that using the longer laser wavelength (1032 nm; green line in Fig 4.) for modulation is disadvantageous below 20 nm, because for this case the length of the nanobunch is almost two times longer than for the shorter wavelength case (516 nm). Therefore this effect reduces the coherence in the radiation process, and the energy for 1032 nm is lower than for 516 nm at 20 nm. Above 60 nm, the energies for the 1032 nm laser are about two times higher, than for the 516 nm wavelength case.

According to the calculations, single-cycle 240-as pulses with 134, 244 and 260 nJ energy can be generated at $\lambda_r = 60$ nm for 516, 800 and 1032 nm modulator lasers, respectively. In the VUV range generation of sub-fs pulses with around half a microjoule energy is possible.

The above discussed robust method for production of CEP-stable, pulse-shape-controlled, linearly polarized attosecond pulses [5, 12, 14], can be easily modified (by using helical undulator) in order to generate circularly polarized attosecond pulses [13]. The electric field of the calculated pulse with this setup is shown in Fig 5. The blue and the green curves are the x and y electric field components, respectively. Using $\lambda_{RU} = 42.6$ cm undulator period and $K = 0.5$ undulator parameter for the RU ($B_0 = 80.1$ mT, $\gamma = 2000$) simulations predict $E_{max} \approx 4$ MV/cm maximum value of the electric field, of the generated 240-as-long EUV pulses.

The main results of the linearly and circularly polarized EUV pulses are summarized in Table 2. The CEP stability of both the linearly and circularly polarised attosecond pulses is better than 50 mrad.

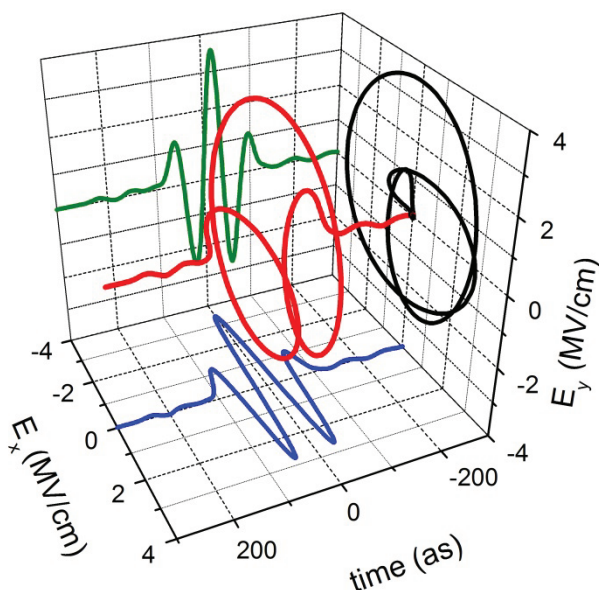


Figure 5: The electric field of the generated few cycle, circularly polarized attosecond pulse (red) and the x (blue) and y (green) components of the field. ($\gamma = 2000$, $K = 0.5$, $\lambda_r = 60$ nm).

Table 2: Summarized Results

Wavelength	Pulse duration	Polarization (C/L)	Energy
20 nm	80 as	Linear	30 nJ
60 nm	240 as	Linear	260 nJ
100 nm	400 as	Linear	360 nJ
20 nm	90 as	Circularly	30 nJ
60 nm	270 as	Circularly	170 nJ
100 nm	450 as	Circularly	300 nJ

CONCLUSION

In summary, practical aspects of the method proposed in our previous work [8,13] for CEP stable linearly and circularly polarized attosecond EUV pulse generation were investigated in detail by means of numerical simulations. The energy of the generated attosecond EUV pulse with various parameters was studied.

Our calculations predict for example single-cycle linearly polarized CEP-stable pulses with 260 nJ energy at 60 nm wavelength and 240 as duration, and circularly polarized pulses with 170 nJ energy at 60 nm wavelength and 270 as duration.

The predicted tens- or hundreds-of-nJ energy of the attosecond pulses enables to use them as pump pulse in pump-probe measurements. Pulses with the predicted exceptional parameters can enable time- and CEP-resolved measurements with sub-100-as resolution.

ACKNOWLEDGMENT

Financial support from Hungarian Scientific Research Fund (OTKA) grant No. 113083 and 101846 is acknowledged. JAF acknowledges support from János Bolyai Research Scholarship (Hungarian Academy of Sciences). The present scientific contribution is dedicated to the 650th anniversary of the foundation of University of Pécs, Hungary.

REFERENCES

- [1] P. Dombi, *J. Mod. Opt.*, **53**, 163-172 (2006) and references therein.
- [2] F. Krausz and M. Ivanov, *Rev. Mod. Phys.* **81**, 163 (2009).
- [3] Y. Jiang et al., *Phys. Rev. Lett.* **105**, 263002 (2010).
- [4] M. Magrakvelidze et al., *Phys. Rev. A* **86**, 013415 (2012).
- [5] A. Marinelli *et al.*, *Phys. Rev. Lett.* **110**, 064804 (2013).
- [6] A. Zholents and G. Penn, *Phys. Rev. ST Accel. Beams* **8**, 050704 (2005)
- [7] D. J. Dunning *et al.*, *Phys. Rev. Lett.* **110**, 104801 (2013).
- [8] Z. Tibai *et al.*, *Phys. Rev. Lett.* **113**, 104801 (2014).
- [9] online at <http://www.pulsar.nl/gpt>
- [10] K. Honkavaara *et al.*, “Status of the FLASH II Project”, in Proceedings of the 34th International Free-Electron Laser Conference, (FEL2012, Nara, Japan, 2012), Report No. WEPD07.
- [11] S. Ackermann *et al.*, “Optimization of HHG Seeding between 10 nm to 40 nm”, in Proceedings of the 34th International Free-Electron Laser Conference, (FEL-2012, Nara, Japan, 2012), Report No. TUPD11.
- [12] Z. Tibai *et al.*, *Phys. Rev. ST Accel. Beams*, submitted.
- [13] Gy. Tóth *et al.*, *Opt. Lett.*, accepted.
- [14] Gy. Tóth *et al.*, “Investigation of novel shape-controlled linearly and circularly polarized attosecond pulse sources”, in Proceedings of the International Workshop on PIPAMON Conference, Debrecen, Hungary, March 2015, submitted.